# Distortions in VSP spectral ratios caused by thin horizontal layering

Albena Mateeva

**ABSTRACT**
The goal of this paper is to put an upper bound on the bias caused by ignored scattering in absorption estimates from VSP spectral ratios in a horizontally layered medium. The most unfavorable situation for absorption estimation is when a strong reflection coefficient series (reflectivity) is over- or underlain by a weak reflectivity. Somewhat extreme, yet realistic examples show that in a strong stationary reflectivity about half of the spectral ratio slope can be due to apparent attenuation (scattering). In a non-stationary reflectivity the influence of scattering is even greater – it can either cause a high-frequency loss larger than anelasticity, or on the contrary, it can over-compensate the anelastic loss and lead to a spectral ratio with a positive slope (negative effective $Q$). The smaller the receiver separation in a non-stationary reflectivity, the larger the bias of the absorption estimate.
In principle, surface-related multiples can contribute to the apparent attenuation by magnifying the thin-layering effects. It turns out, however, that their influence is negligible at the early times typically used in VSP spectral ratios for absorption estimation.

**Key words:** layered media, attenuation, scattering, Q, borehole geophysics, exploration seismology

## 1 INTRODUCTION

In exploration seismology, absorption estimates come largely from Vertical Seismic Profile (VSP) experiments. The most popular techniques are based on spectral ratios, i.e., comparing the frequency content of the first arrival at successive receiver locations (different VSP methods for absorption estimation are discussed in Tonn, 1991; for a more recent development see, for example Sun & Castagna, 2000).

Unfortunately, VSP spectral ratios can be contaminated by frequency-dependent scattering from small-scale heterogeneities in the medium (e.g., thin layers). Thus, these ratios measure the effective attenuation, which is a biased estimate of the intrinsic absorption. The goal of this paper is to assess the maximum share of apparent attenuation that can be introduced in the effective attenuation estimates by thin horizontal layering. I assume that the effective attenuation is derived from noise-free VSP spectral ratios (no background noise, timing and positioning errors, etc.).

I start by reviewing some properties of the earth reflection coefficient series (which I call "reflectivity" for short) that determine the spectral coloring of the impulse response in the absence of absorption. Then I explain the frequency content of the elastic$^\star$ spectral ratios. Contrary to popular belief, they are not necessarily high-frequency deficient in the presence of thin layering; i.e., ignoring scattering does not necessarily lead to an overestimate of the intrinsic absorption. I take into account the presence of the earth surface, which magnifies the thin-layering effects. After having identified the most unfavorable geological settings for absorption estimation, I quantify the bias (the apparent attenuation, or the difference between effective and intrinsic attenuation) that can be expected in such settings through a couple of synthetic, yet realistic examples. I show that when the subsurface is characterized by a strong and stationary reflection coefficient series,

$^\star$Throughout this paper "elastic" refers to the lack of absorption, not to the presence of shear-waves.

the elastic VSP spectral ratios exhibit apparent attenuation comparable to that caused by absorption in a medium with $Q_{int} = 70$. The largest bias, though, is likely to occur when geology changes with depth. In a non-stationary reflectivity, scattering can either cause an even greater high-frequency loss than intrinsic absorption or, on the contrary, it can over-compensate for the anelastic loss and lead to spectral ratios with a positive slope (negative effective $Q$, the qaulity factor being defined as $Q = -20\pi \log e/slope \approx -27/slope$).

## 2 EARTH REFLECTIVITY

Two characteristics of a reflectivity series govern the seismic trace spectrum. The first is the magnitude of the reflection coefficients, which determines how energetic the multiples will be compared to the primaries. The second is the frequency content of the reflection coefficient series. Typical earth reflectivities are approximately frequency-independent (pseudo-white) only above a corner frequency, below which their power spectra fall as $f^{\beta}$, $\beta \in [0.5; 1.5]$ (Walden & Hosken, 1985; Saggaf & Robinson, 2000). The stronger the deviation of a reflectivity from whiteness, the stronger the coloring (the frequency-dependance) in its impulse response.

The magnitude and frequency content of a reflection coefficient series are not completely independent characteristics because the acoustic impedance of the subsurface can vary only within certain limits. Strong reflectivities have markedly "blue" spectra, i.e., spectra whose power increases with frequency over most of the seismic frequency band. In such blue sequences, closly spaced samples are negatively correlated; i.e., consecutive reflection coefficients tend to have the opposite sign. This is the only way to have a large number of large reflection coefficients while the acoustic impedance stays within certain geological bounds.

## 3 RECEIVER IN A LAYERED HALF-SPACE

Strong reflectivities are of primary interest to this study because they are likely to cause problems with absorption estimation. However, to understand how thin layering acts on the signal in a down-hole receiver, it is instructive to look first at a simple weak-reflectivity approximation.

Suppose $R(\omega)$ is the Fourier transform of the time-domain reflection coefficient series (reflectivity log). As discussed in the previous section, $R(\omega)$ is an increasing function of frequency. For now assume that the thin layering is stationary, so that $R(\omega)$ does not change with depth (the non-stationary case will be considered later). Using the results of Banik *et al.*, 1985 [namely, their eqs. (17) and (25)] one can show that near the time $T$ of the direct arrival the impulse response $p$ at a buried receiver is

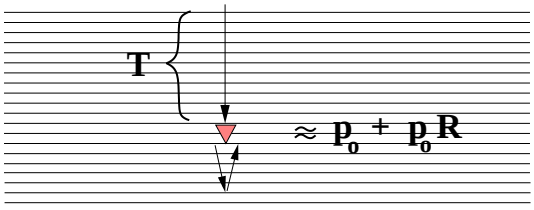


**Figure 1.** Signal in a buried receiver: transmitted train ($p_0$) and its primary reflections from below ($p_0R$); multiples of the reflections from below are ignored.

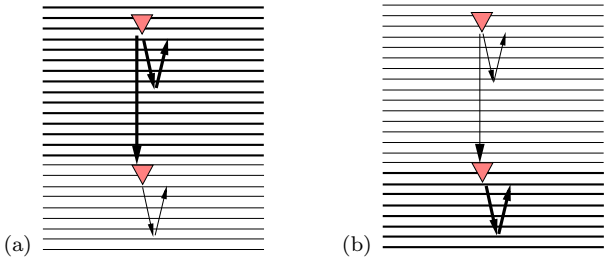


**Figure 2.** VSP in a non-stationary reflectivity: (a) strong above weak reflectivity; (b) weak above strong reflectivity. Thick arrows indicate arrivals that contribute significantly to the signal coloring; thin arrows represent weak contributions or weak filtering.

$$p(\omega) \approx p_0(\omega)\,(1 + R(\omega))\,, \tag{1}$$

where $p_0$ is the transmission impulse response of a stack of layers with a (one-way) traveltime thickness $T$. The transmission impulse response $p_0$ is minimum-phase, with an amplitude spectrum given by O'Doherty & Anstey's formula (O'Doherty & Anstey, 1971)

$$|p_0(\omega)| = e^{-|R(\omega)|^2\,T}\,, \tag{2}$$

where $T$ is dimensionless (normalized by the time-thicknes of an individual thin layer, i.e., the sampling interval of the time-domain reflection coefficient series).

Equation (1) tells us that in a small window after the first break, the main contributions to the trace come from the transmitted impulse (filtered by the overburden) and its primary reflections from the interfaces immediately below the receiver location (Fig. 1). This is a weak-reflectivity approximation because it ignores multiples of the reflections from below the receiver as well as changes, over the considered time window, in the downgoing pulse that generates them. Equations (1) and (2) might be numerically inaccurate for strong reflectivities but they capture the most important facts (remember $R(\omega)$ is blue):

(i) the transmission through the layered overburden causes apparent loss of high frequencies ("apparent attenuation");

(ii) the reflections from immediately below the receiver boost the high-frequency content of the trace near the first arrival.

These counter-actions determine the final "color" of the trace at the early times typically used in VSP spectral ratios for absorption estimation. In a stationary reflectivity, the reflections from below have the same relative contribution at any receiver. Thus, the elastic spectral ratios exhibit apparent attenuation purely due to the transmission through the stack of layers between the receivers.

In practice, reflectivities are often non-stationary and the reflections from below play an important role in the spectral ratios. We can consider two basic situations: weak reflectivity above strong reflectivity and vice versa. First, suppose the shallower receiver is in a strong reflectivity zone and the deeper receiver is underlain by a weak reflectivity (Fig. 2a). The signal in the deeper receiver has not only been depleted of high frequencies during transmission, it also lacks the high-frequency boost that would have been provided by reflections from below. Therefore, the spectral ratio between the two receivers will exhibit an even larger apparent attenuation than that in a strong but stationary reflectivity. Now let the geometry be reversed (Fig. 2b); in this case the high-frequency boost by reflections from below in the deep receiver is much larger than that in the shallow one and can even overcome the (small) high-frequency loss along the path between the receivers. Thus, the signal may appear to enrich in high-frequencies with depth. If the absorption of the medium is too small to overturn the slope of the elastic spectral ratio, we may observe a negative effective $Q$. Negative effective $Q$ values have been reported in the literature (De *et al.*, 1994; @warning Citation '*VSPwQ' on page 3 undefined).

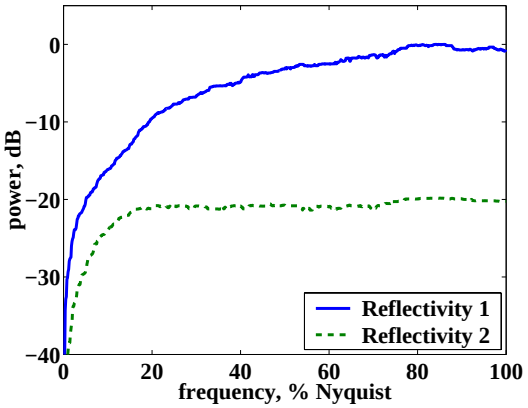


**Figure 3.** Power spectrum of the synthetic reflection coefficient series: Reflectivity 1 is strtong and blue, Reflectivity 2 is weak and almost white.

| | Reflectivity 1 (strong, blue) | Reflectivity 2 (weak, almost white) |
|---|---|---|
| $\theta$ | 0.9 | 0.98 |
| $\phi$ | 0.3 | 0.8 |
| mean | -0.0002 | -0.0002 |
| std | 0.11 | 0.02 |
| p | 1.0 | 0.23 |
| $\lambda_1$ | 0.09 | 0.007 |
| $\lambda_2$ | — | 0.017 |

**Table 1.** The two synthetic reflectivities used throughout the examples are modelled as ARMA(1,1) processes with autoregressive parameter $\theta$ and moving average parameter $\phi$. The amplitudes of the reflection coefficients are drawn from a mixture of two Laplace distributions with a mixing proportion parameter $p$ and scale parameters $\lambda_1$ and $\lambda_2$, respectively (Appendix A).

## 4 INFLUENCE OF THE FREE SURFACE

The previous section was devoted to the spectral coloring caused by thin layering alone. The presence of the earth surface was not taken into account.

The main role of the earth surface (a free surface) is to retain in the medium whatever frequencies have reached it and put them back in circulation. How much a trace would be influenced by these re-introduced frequencies depends on the receiver depth. A shallow receiver would feel the surface-related multiples at all frequencies. Since in a blue reflectivity sequence the depth of penetration (the localization length) decreases with frequency, only a small portion of the high frequencies bounced back by the earth surface would reach a downhole receiver. Thus, the deeper the receiver, the narrower (lower) the frequency band over which surface-related multiples add to the trace. This, combined with the fact that a low enough frequency contributes equally to all traces (all receivers become "shallow" compared to the localization depth as $\omega \to 0$), may cause additional apparent attenuation in VSP spectral ratios. The effect is stronger at later times when surface-related multiples make a larger difference on the trace than they do at early times (see the example below).

## 5 END-MEMBER EXAMPLES

The purpose of this section is to illustrate the above concepts and to put an upper bound on the bias of the absorption estimates derived from VSP spectral ratios in finely layered media.

I compute VSP spectral ratios for horizontally layered, perfectly elastic earth models and compare them to the ratios expected in a homogeneous but anelastic space. In media with spatially-invariant absorption properties, the total attenuation is a simple superposition of scattering effects and intrinsic absorption, so the comparison between their individual values makes sense.

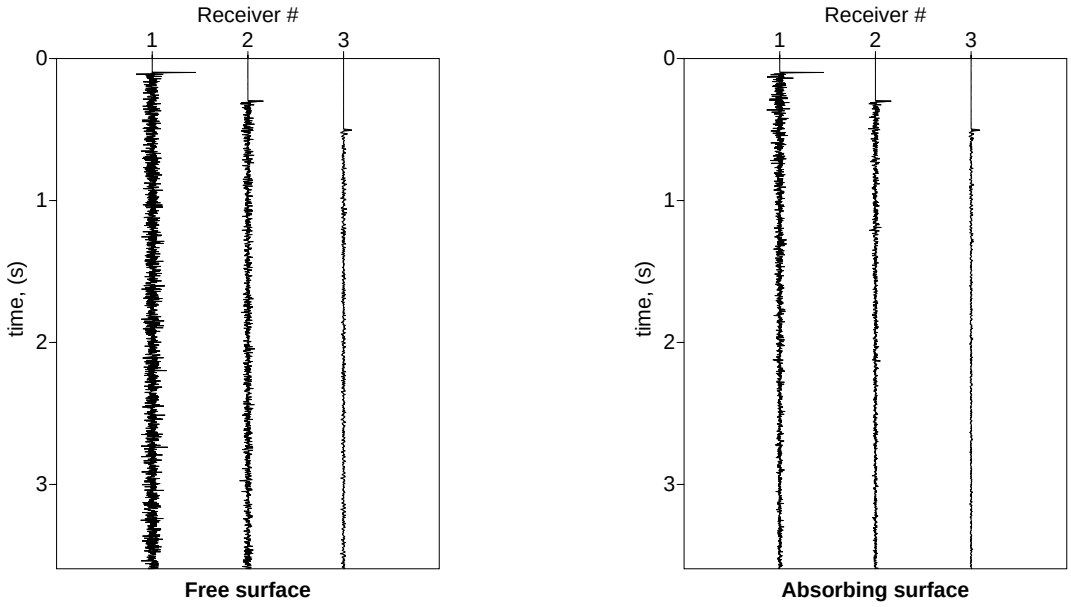


(a) (b)

**Figure 4.** VSP elastic impulse response in a strong stationary reflectivity: (a) with surface-related multiples (as are traces recorded in practice); (b) without surface-related multiples (shown for comparison). The receivers are 200 ms apart (200 layers apart in the Goupillaud model – Appendix A), the first being at 100 ms (100 layers) below the earth surface.

My computations (by a time-domain reflectivity code with a Goupillaud model – Appendix A) are for plane waves at normal incidence but the results are directly applicable to a zero-offset VSP with a point source because the geometrical spreading will introduce only a frequency-independent scaling factor in the spectral ratios (e.g., Asch *et al.*, 1991).

I first consider the case of a stationary, strong reflectivity. Then I append the strong reflectivity, above or below, with a much weaker one to create extreme examples of non-stationary layering.

My reflection coefficient series are synthetic but realistic, similar to those of Well 8 and Well 5 from the papers of Walden and Hosken (1985, 1986). Their properties are given in Table 1, and their power spectra are depicted in Fig. 3. The generation of the reflectivities is described in Appendix A.

### 5.1 Strong stationary reflectivity

The normal-incidence elastic impulse response of Reflectivity 1 is shown in Fig. 4 for three down-hole receivers. The loss of high frequencies with depth is clearly seen in the first-arrival zoom in Fig. 5 and in the spectra in Fig. 6. The spectral ratio between the early events on the deepest and the shallowest trace (Fig. 7a, solid line) has a slope of -0.4 dB/Hz/s. It is comparable to the slope produced by intrinsic absorption in a homogeneous medium with intrinsic quality factor $Q_{int} = 70$.

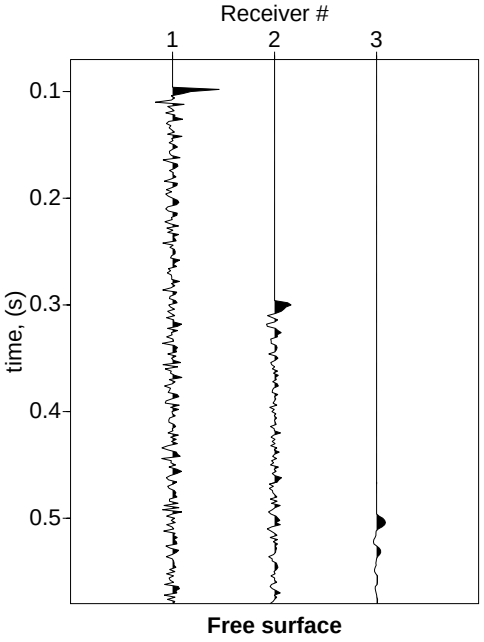


**Figure 5.** Zoom from Fig. 4a: The transmitted train disperses and loses high-frequencies with depth.

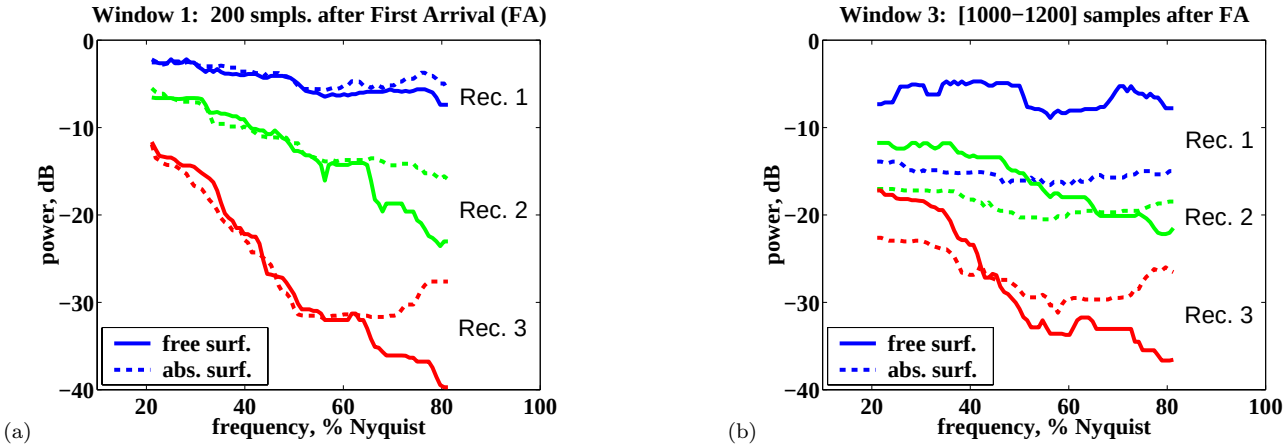


**Figure 6.** Power spectra at three receiver depths with and without surface-related multiples: (a) At early times, surface-related multiples have negligible influence on trace spectra, except at high frequencies, which are rarely used in absorption estimation. (b) At late times, surface-related multiples make spectra of down-hole traces steeper, amplifying the loss of high frequencies with depth.

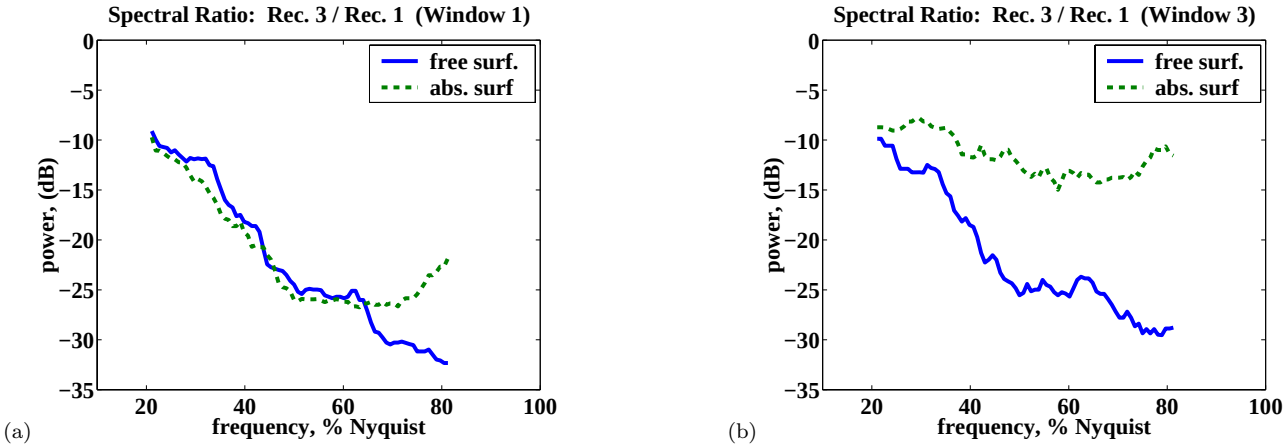


**Figure 7.** Spectral ratio between Receiver 3 and Receiver 1 (400 ms apart): (a) at early times; (b) at late times. Note that the slope of the solid lines is essentially same in (a) and (b).

Therefore, in a stationary reflectivity, about half of the observed spectral ratio slope (absorption and apparent attenuation together) may come from apparent attenuation. It is due mainly to the thin layering between the receivers – the additional apparent attenuation caused by surface-related multiples is insignificant at early times (Figs. 6a, 7a). Surface-related multiples become important later on the trace (Fig. 6b, 7b). This is easy to understand if we compare the traces with and without surface-related multiples in the time domain (Fig. 4a,b). In the presence of a free surface, down-hole traces become stationary after the transmission train has passed. Without the free surface, traces decay with time. Thus, at late times, the traces that we record in the field consist largely of surface-related multiples, even though the early portions of the traces with and without a free surface are quite similar. This means that while spectral ratios obtained from early windows carry information about the medium between the receivers, ratios based on late windows would be strongly influenced by the properties of the near surface. It should be pointed out that regardless of the dominant mechanism, the apparent attenuation does not change with time in a stationary reflectivity (Fig. 7), at least over the lower half of the trace spectrum, typically used for absorption estimation for its high signal-to-noise ratio.

Another feature of the apparent attenuation in a stationary reflectivity is that it does not depend on the receiver separation – only the uncertainty of its estimate increases as the receivers get closer (Fig. 8). As we will see, this is not the case in a non-stationary reflectivity, where an elastic spectral ratio depends on the contrast in the reflectivity properties beneath the two receivers, which is a factor not proportional to receiver separation.

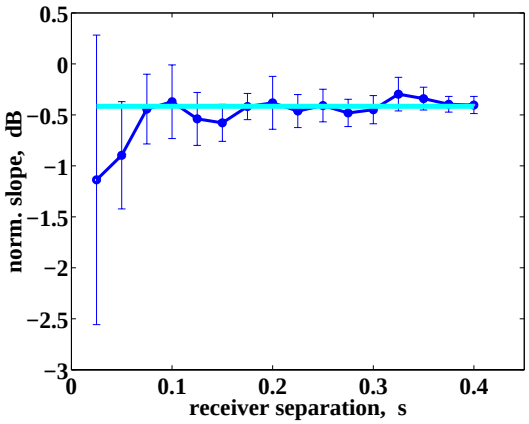


**Figure 8.** Slope of the spectral ratio between Receiver 3 and a number of shallower receivers, normalized by the one-way traveltime between the receivers in a strong stationary reflectivity. The time window for spectral estimation is 256 samples long. The spectra on all traces were smoothed by a 20% median filter before computing the spectral ratios. The error bars represent the uncertainty of each slope estimate (least-squares fit). The data are compatible with a constant apparent attenuation (thick gray line – computed by weighted least-squares).

The increased variability of the slope estimates from close receivers in Fig. 8 is caused by the inability of the down-going pulse to stabalize (self-average while propagating through the scattering medium) over the short path of propagation between the receivers. Shapiro and Zien (1992) showed that, for a purely transmissional experiment (no reflections from below a receiver), the standard deviation of the estimated apparent attenuation $\alpha$ is

$$\sigma_\alpha \propto \sqrt{\frac{\alpha}{L}}\,, \tag{3}$$

where $L$ is the distance traveled, i.e., the distance between the receivers. The closer the receivers, the larger the uncertainty $\sigma_\alpha$. In our experiment, reflections from below the receivers also contribute to the variability of the attenuation estimate, and their contribution does not diminish as the receiver separation increases (they do not self-average). That is why, the apparent attenuation uncertainty does not vanish for large receiver separations. The data in Fig. 8 are consisten with the observation of Spencer *et al.* (1982) that there is an "optimal" receiver separation for attenuation estimation – below it the variability of the estimates is too large; beyond it the variability does not decrease substantially with distance.

### 5.2 Strong above weak reflectivity

The largest apparent attenuation occurs in a non-stationary reflectivity when the deeper receiver is underlain by a weak reflectivity. To simulate such a case, I appended the strong, blue Reflectivity 1 by the weak, almost white Reflectivity 2 at the level of Receiver 3 (500 layers below the earth surface). The elastic impulse responses in Receiver 1 (in the strong reflectivity zone) and Receiver 3 (just below the strong reflectivity) are shown in Fig. 9a, and their spectra at early times are shown in Fig. 10a. The spectra do not look much different from those in the stationary case, just their ratio (Fig. 11a) is about -0.02 dB/Hz steeper than before[†]. This increase in slope, however, occurs "instantly" across the reflectivity jump; it is determined purely by the contrast in the reflectivity properties below the two receivers, and does not depend on the receiver separation (given that Receiver 3 stays in place, so that the path between the receivers is entirely in Reflectivity 1). Thus, while this additional apparent attenuation caused by change in geology will be small compared to the total attenuation accumulated along the path between distant receivers, it can contribute significantly to absorption estimates[‡] extracted from close receivers. Of course, in practice, the slope of the spectral ratio is not discontinuous at the depth of the reflectivity change because of the finite time-window used for spectral estimation; as the receivers get closer together, the window around the first arrival on the shallow trace starts to sample the weak reflectivity zone. Despite this smearing though, the total apparent attenuation can exceed the attenuation due to absorption for $Q_{int} = 50$ when the receiver separation is less than 220 ms. This is illustrated in Fig. 12 shows the spectral ratio between Receiver 3 and a number of shallower receivers, normalized by the traveltime between the receivers in a pair. Now, unlike in the stationary reflectivity case in Fig. 8, the data are incompatible with a constant apparent attenuation but are consistent with a linear model, i.e., apparent attenuation linearly dependent on receiver separation. As the receiver offset decreases, the apparent attenuation increases.

### 5.3 Weak above strong reflectivity

Now let the weak Reflectivity 2 be underlain by the strong Reflectivity 1, and again let the change occur at the depth of Receiver 3. The elastic impulse response, shown in Fig. 9b, is more dynamic than in the previous case. The weak scattering in the overburden leaves the transmitted signal much stronger and more compact (compare with Fig. 9a; all traces are plotted on the same scale). The reflection from the top of the strong-reflectivity zone is seen in Receiver 1 at 0.9 s. The event

[†]Note that the change of slope here is given in dB/Hz; it is not normalized by the time-separation between Receivers 1 and 3.

[‡]Absorption estimates are based on spectral ratios slopes, normalized by receiver separation, e.g., dB/Hz/s=dB.

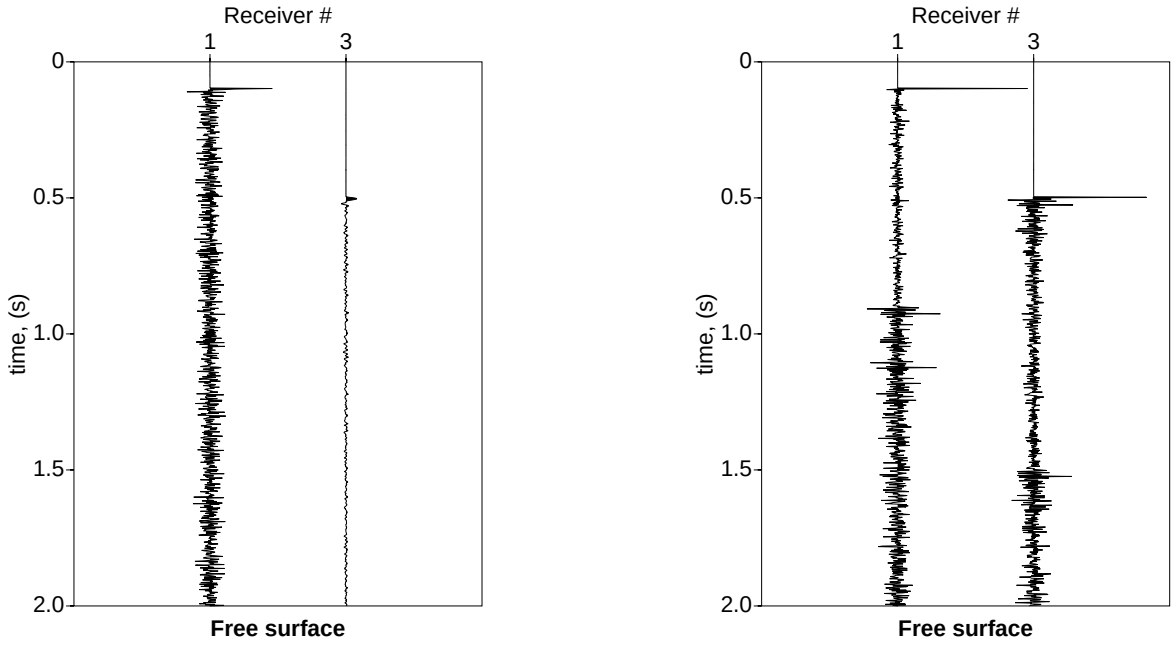


(a) (b)

**Figure 9.** VSP elastic impulse response with surface-related multiples in (a) strong-above-weak reflectivity; (b) weak-above-strong reflectivity. The receiver placement and numeration is as in Fig. 2. The receiver depths are the same as in the stationary case – 100 ms and 500 ms below the surface, respectively.

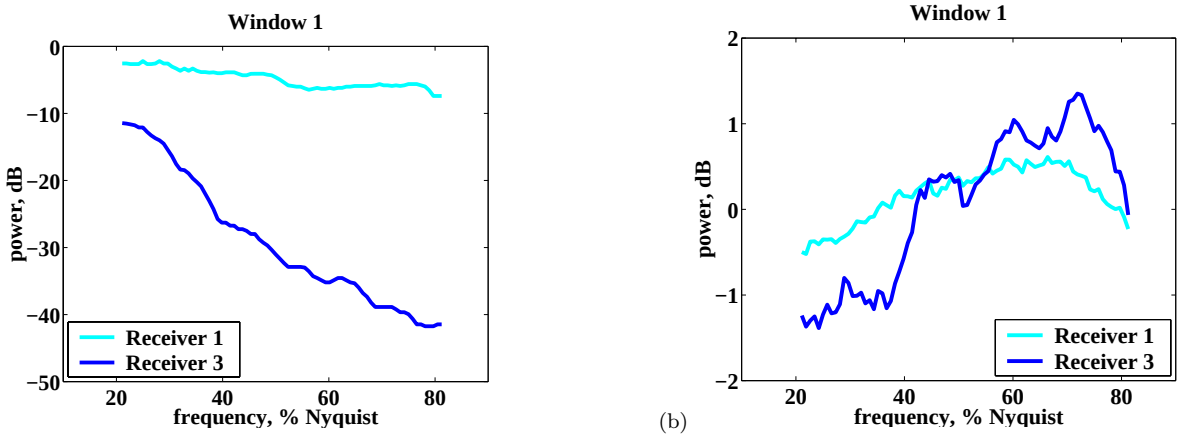


(a) (b)

**Figure 10.** Elastic spectra at early times (Window 1: 200 samples after the first arrival) in (a) strong-above-weak reflectivity; (b) weak-above-strong reflectivity.

at 1.1 s is its free-surface multiple. This free-surface multiple is also seen at 1.5 s in Receiver 3. Before that, the trace decays with time as it would in the absence of a free surface because the surface-related multiples of the reflections generated in the overburden are too weak to compensate for the transmission losses in the strong reflectivity below the receiver. The surface-related multiples of the reflections from the strong reflectivity zone noticeably boost the energy in Receiver 3 after 1.5 s.

The early-time spectra of the two traces are shown in Fig. 10b. The spectrum of the shallow trace is slightly blue because the reflections from below, even though weak, outweigh the filtering in the overburden, i.e., the $(1 + R)$ term in eq. (1) over-compensates the high-frequency deficit in $p_0 = \exp(-T|R|^2)$ at the depth of Receiver 1. The over-compensation is even more dramatic in Receiver 3 for which the former term contains the strong and blue Reflectivity 1 and the later term

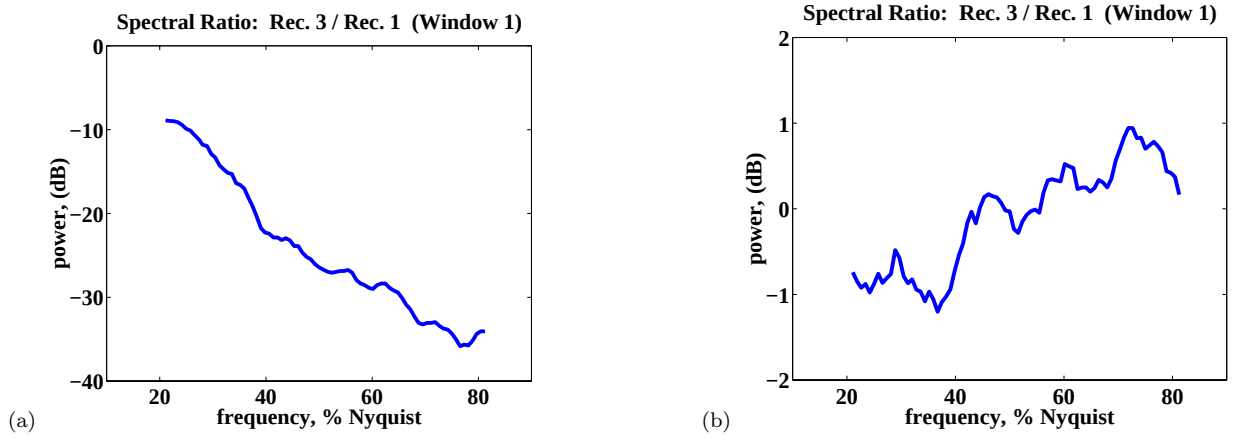


**Figure 11.** Spectral ratio in (a) strong-above-weak reflectivity; (b) weak-above-strong reflectivity.

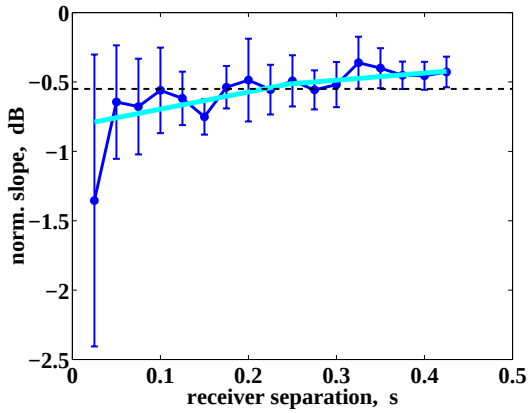


**Figure 12.** Analogous to Fig. 8 but for the strong-above-weak reflectivity case. The thick gray line is the best weighted-least-squares fit and actually consists of two independently estimated segments – one for large receiver separation such that the time-window on the shallow trace does not sense the weak reflectivity below the deeper receiver, and another for smaller separation. The two segments give virtually identical estimates for the apparent attenuation trend. The thin dashed line indicates the slope produced by intrinsic absorption in a medium with $Q_{int} = 50$.

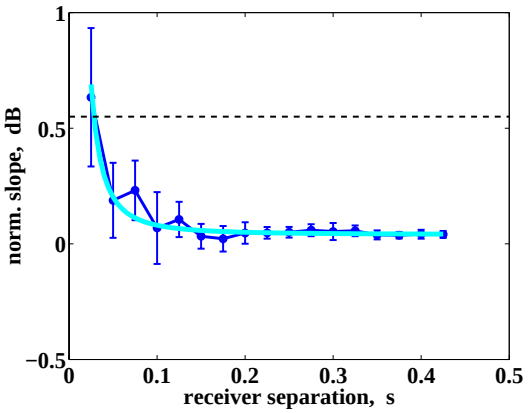


**Figure 13.** Analogous to Fig. 8 but for the weak-above-strong reflectivity case. The thin dashed line indicates the absolute value of the slope produced by intrinsic absorption in a medium with $Q_{int} = 50$.

contains the weak, almost white Reflectivity 2. Thus, the signal in the deep receiver is richer in high frequencies than the signal in the shallower receiver. This leads to a spectral ratio with a positive slope (Fig. 11b). The slope is only about 0.015 dB/Hz but since it occurs instantly across the reflectivity change (as explained in the previous section) it can be large compared to that attributable to intrinsic absorption when the receivers are close. This is illustrated in Fig. 13. It shows the spectral ratio between Receiver 3 and a number of shallower receivers, normalized by the receiver pair separation. The apparent gain of high frequencies with depth increases inversely proportional to the square of the receiver separation (that is the lowest order polynomial that fits the trend). For a receiver separation of less than 30 ms, scattering can over-compensate for the high-frequency loss caused by anelasticity in a medium with $Q_{int} = 50$ and produce a negative effective $Q$.

A comparison between the intrinsic and effective $Q$, summarizing the examples from this section is given in Table 2.

## 6 CONCLUSIONS

Based on the above most unfavorable, yet realistic examples, we can conclude the following:

(i) To characterize the medium between two receivers, one can use early windows on VSP traces (the data at early times are almost uncontaminated by surface-related multiples).

(ii) In a stationary reflectivity, VSP spectral ratios exhibit apparent attenuation comparable to that caused

| | $Q_{int}$ | $Q_{eff}$ dt=200 ms | $Q_{eff}$ dt=20 ms |
|---|---|---|---|
| 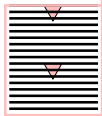 | 50 | 30 | 30 |
| 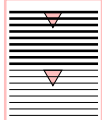 | 50 | 25 | 20 |
|  | 50 | 55 | negative |

**Table 2.** Effective versus intrinsic $Q$ for end-member reflectivity examples. Shown are estimates of $Q_{eff}$ from receiver pairs with large and small separation (e.g., $dz = 500$ m and $dz = 50$ m in a medium with velocity 2500 m/s).

by absorption in a homogeneous medium with $Q_{int} = 70$.

(iii) The largest apparent attenuation occurs when the shallow receiver is in a strong reflectivity zone and the deep receiver is underlain by a weak reflectivity. In such cases the apprent attenuation dominates the VSP spectral ratio, unless the receiver separation is large (e.g., more than 220 ms in a medium with an intrinsic $Q_{int} = 50$).

(iv) A negative effective $Q$ (spectral ratio with a positive slope) can be observed when the shallow receiver is in a weak reflectivity and the deep receiver is underlain by a strong reflectivity, and the receiver separation is small (e.g., less than 30 ms in a medium with an intrinsic $Q_{int} = 50$).

Common wisdom tells us that absorption cannot be reliably assessed from spectral ratios between closly spaced receivers because the variability of the slope estimate is large compared to the slope itself. The fact that scattering tends to bias absorption estimates more when the receivers are close is an additional reason not to use close pairs.

To assess intrinsic absorption (anelasticity) from VSP spectral ratios, we need sonic and density logs from which to predict the scattering effects.

## REFERENCES


Asch, M., Kohler, W., Papanicolaou, G., Postel, M., & White, B. 1991. Frequency Content of Randomly Scattered Signals. *SIAM Review*, **33**(4), 519–625.

Banik, N.C., Lerche, I., & Shuey, R.T. 1985. Stratigraphic Filtering, Part I: Derivation of the O'Doherty-Anstey Formula. *Geophysics*, **50**, 2768–2774.

Cohen, J. K., & Stockwell, Jr. J. W. 2002. *CWP/SU: Seismic Unix Release 36: a free package for seismic research and processing*. Colorado School of Mines.

De, G. S., Winterstein, D. F., & Meadows, M. A. 1994. Comparison of P- and S-wave velocities and Q's from VSP and sonic log data. *Geophysics*, **59**(10), 1512–1529.

Ganley, D. C. 1981. A Method for Calculating Synthetic Seismograms Which Include the Effects of Absorption and Dispersion. *Geophysics*, **46**, 1100–1107.

O'Doherty, R. F., & Anstey, N. A. 1971. Reflections on Amplitudes. *Geophys. Pros.*, **19**, 430–458.

Robinson, E. A. 1983. *Multichannel Time Series Analysis with Digital Computer Programs*. 2 edn. Goose Pond Press.

Saggaf, M. M., & Robinson, E. A. 2000. A United Framework for the Deconvolution of Traces of Nonwhite Reflectivity. *Geophysics*, **65**, 1660–1676.

Shapiro, S. A., & Zien, H. 1992. Transmission of wavefields through finely layered media: attenuation, velocity, fluctuations. *Pages 820–823 of: SEG Ann. Int. Mtg. Expanded Abstracts*.

Spencer, T. W., Sonnad, J. R., & Butler, T. M. 1982. Seismic Q – Stratigraphy or Dissipation. *Geophysics*, **47**, 16–24.

Sun, S., & Castagna, J. 2000. Attenuation Estimation from Vertical Seismic Profile Data. *Pages 1787–1790 of: 70-th Ann. Intern. Mtg. of SEG – Expanded Abstracts*, vol. 70. SEG.

Tonn, R. 1991. The Determination of the Seismic Quality Factor Q from VSP Data: A comparison of Different Computational Methods. *Geophys. Pros.*, **39**, 1–27.

Walden, A. T. 1993. Simulation of Realistic Synthetic Reflection Sequences. *Geophys. Pros.*, **41**, 313–321.

Walden, A. T., & Hosken, J. W. J. 1985. An Investigation of the Spectral Properties of Primary Reflection Coefficients. *Geophys. Pros.*, **33**, 400–435.

Walden, A. T., & Hosken, J. W. J. 1986. The Nature of Non-Gaussianity of Primary Reflection Coeficients and Its Significance for Deconvolution. *Geophys. Pros.*, **34**, 1038–1066.


## APPENDIX A: COMPUTATIONAL NOTES

This appendix describes how synthetic reflectivities and synthetic seismograms were generated.

### A1 Reflection coefficient series

A time-domain synthetic reflectivity $\{r_i\}$ can be modeled as an ARMA(1,1) process (Walden & Hosken, 1985) with an autoregressive parameter $\theta$ $(0 < \theta < 1)$ and a moving average parameter $\phi$ $(0 < \phi < 1, \phi < \theta)$, i.e.,

$$r_i = \phi\, r_{i-1} + a_i - \theta\, a_{i-1}\,, \qquad \text{(A1)}$$

where $\{a_i\}$ is an independent and identically distributed (*iid*) innovation sequence. The larger the difference between $\theta$ and $\phi$, the steeper with frequency (more "blue") is the power spectrum of the reflectivity. These two parameters define the *correlation* between the samples in the time-domain reflectivity $\{r_i\}$.

The *amplitudes* of the reflection coefficients follow a mixture of two Laplace distributions with a mixing

proportion parameter $p$ ($0 \le p \le 1$ being the proportion of the first distribution) and scaling parameters $\lambda_1$ and $\lambda_2$, respectively (Walden & Hosken, 1986). These three quantities define the variance $\sigma_r^2$ and the kurtosis $K_r$ of the reflectivity series ($K_r > 6$, as found out by Walden and Hosken by analyzing well-logs from various locations).

To generate a time series $\{r_i\}$ with the desired correlation, variance and kurtosis, the innovation sequence $\{a_i\}$ in eq. (A1) is drawn from a mixed Laplace distribution with variance $\sigma_a^2$ and kurtosis $K_a$ such that

$$\sigma_a^2 = \frac{1-\phi^2}{1+\theta^2-2\phi\theta}\,\sigma_r^2 \tag{A2}$$

$$K_a = \left[K_r - 6\,\frac{(\phi-\theta)^2\,(1-\phi^4)+\phi^2\,(\phi-\theta)^4}{\left[1-\phi^2+(\phi-\theta)^2\right]^2\,(1+\phi^2)}\right]\cdot \frac{\left[1-\phi^2+(\phi-\theta)^2\right]^2\,(1+\phi^2)}{\left[1-\phi^4+(\phi-\theta)^4\right]\,(1-\phi^2)} \tag{A3}$$

The connection between the variance $\sigma^2$ and the kurtosis $K$ of a Laplace mixture, and the distribution parameters $p$, $\lambda_1$, $\lambda_2$ is

$$\sigma^2 = 2\,\left(\,p\,\lambda_1^2 + (1-p)\,\lambda_2^2\,\right)\,, \tag{A4}$$

$$K = 6\,\frac{p\,\lambda_1^4 + (1-p)\,\lambda_2^4}{p\,\lambda_1^2 + (1-p)\,\lambda_2^2} \tag{A5}$$

Given the desired variance and kurtosis for the sequence $\{a_i\}$ [eqs. (A2),(A3)], the relationships (A4)–(A5) are insufficient to determine $p_a$, $\lambda_{a1}$, $\lambda_{a2}$ (three unknowns). As an additional constraint, one may require that $\lambda_{r1}/\lambda_{r2} = \lambda_{a1}/\lambda_{a2}$. It has been observed that in most cases $\lambda_{r2} \approx 3\lambda_{r1}$ (Walden & Hosken, 1986). Even with this restriction, however, equations (A4) and (A5) have two plausible solutions for $\{p_a,\, \lambda_{a1},\, \lambda_{a2}\}$ (because of the powers at which $\lambda_1$ and $\lambda_2$ appear in eqs. (A4)–(A5)). Typically, one of the solutions is close to the reflectivity parameters $\{p_r,\, \lambda_{r1},\, \lambda_{r2}\}$; that's the solution I chose.

Once the parameters $\{p_a,\, \lambda_{a1},\, \lambda_{a2}\}$ have been chosen, two *iid* sequences $\{a1_i\}$ and $\{a2_i\}$ are drawn from Laplace distributions with mean zero and scale parameters $\lambda_{a1}$ and $\lambda_{a2}$ respectively. Also, a "flag" sequence $\{b_i\}$ is drawn from a Bernoulli distribution with mean $p_a$. When $b_i = 1$, $a_i = a1_i$; when $b_i = 0$, $a_i = a2_i$. Constructing such an innovation sequence $\{a_i\}$ is easily done, for example, in *Mathematica*.

Having $\{a_i\}$, $\theta$ and $\phi$, we are almost ready to construct the reflectivity $\{r_i\}$ from eq. (A1). We only need an initial value $r_1$ for the reflectivity. Walden (1993) proved that an almost immediate stationarity of the generated reflectivity is provided by the initial conditions:

$$r_1 = \sigma_r e_1 \tag{A6}$$

and

$$a_1 = \frac{\sigma_a^2}{\sigma_r}\,e_1 + \sqrt{\sigma_a^2 - \frac{\sigma_a^4}{\sigma_r^2}}\,e_2\,, \tag{A7}$$

where $e_1$ and $e_2$ are drawn from a mixed Laplace distribution with variance one and mean zero. As the innovations $\{a_i\}$ are independent, the first value $a_1$ can be simply set to (A7).

Since the synthetic reflectivity $\{r_i\}$ was generated with a zero mean, a DC-component $\bar{r}$ can eventually be added to it. The mean $\bar{r}$ of a reflection coefficient log is usually very small (i.e., $\bar{r} \ll \sigma_r$).

The generated reflection coefficients should be checked for physical feasibility (occasionally $|r_i| \le 1$ might be violated, especially when $\sigma_r^2$ is large). I clipped values with magnitude above 0.4.

### A2 Synthetic seismograms

Synthetic seismograms (1D; all multiples included) were computed by the code *sugoupillaud*, freely distributed through the Seismic Unix package (Cohen & Stockwell, 2002). The computations are performed through $z$-transforms (Robinson, 1983; @warning Citation 'nfunds*' on page 10 undefined; Ganley, 1981). The medium is assumed to be lossless and horizontally layered, and is described by a reflection coefficient series $\{r_i\}$ (equi-spaced in time, or, Goupillaud-type layering). The source is a unit spike at time zero; it generates vertically-propagating plane waves. The source can be buried at any depth, though for the purposes of this paper, it was always at the earth surface. A receiver can be placed at any depth. It can measure either a vector-type field (displacement/velocity/acceleration), or pressure. The synthetic seismograms in this paper are for a vector field (e.g. displacement). Further details about the code can be found in its self-documentation.